

# Updated Constraints on Self-Interacting Dark Matter from Supernova 1987A

Cameron Mahoney,<sup>1,\*</sup> Adam K. Leibovich,<sup>1,†</sup> and Andrew R. Zentner<sup>1,‡</sup>

<sup>1</sup>*Pittsburgh Particle Physics Astrophysics and Cosmology Center (PITT PACC)*

*Department of Physics and Astronomy, University of Pittsburgh, Pittsburgh, Pennsylvania 15260, USA*

Abstract?

## I. INTRODUCTION

A nearly overwhelming preponderance of observational evidence indicates that a form of nonrelativistic, non-baryonic, dark matter constitutes the vast majority of mass in the Universe and drives the formation of cosmic structure. The pace of the quest to identify the dark matter is accelerating on many fronts. Weakly-interacting massive particles (WIMPs) have received the most attention as dark matter candidates (see Ref. [1] for a review). Dark matter particles that interact with standard model particles only weakly, while interacting among themselves much more strongly have been studied as an alternative to WIMP scenarios in many contexts [2–16] **[ARZ: Need to add some more recent references here.]** and constraints on self-interacting dark matter (SIDM) models have been explored by many authors [17–33]. In this paper, we revisit and update astrophysical constraints on SIDM models from supernova cooling, finding constraints that are considerably less restrictive than in previous work. **[ARZ: Might want to add a comment about SIDM affecting small-scale structure in CDM, the satellites problems and core/cusp problems.]**

SIDM models in which large self-interaction cross sections are mediated by sufficiently light bosons ( $M \lesssim 100$  GeV) can be constrained astrophysically using supernovae, particularly SN1987A. Light gauge bosons will be produced within the hot supernovae core and radiated from the supernova. This non-standard energy loss mechanism can result in an energy loss rate from the supernova core that is inconsistent with observations of SN1987A, analogous to the classic constraint on axions [34]. This mechanism was already exploited by [35] (and [36], with a slight modification) (**[ARZ: Cameron, add others of which you may be aware.]**) to constraint dark electromagnetism models of SIDM in which the self-

interaction arises from a Yukawa potential and the vector boson is kinetically mixed with the standard model photon.

As we mentioned above, we find SN1987A constraints on dark photon SIDM models that are considerably different from those of [35]. If correct, our result has important consequences. The Snowmass white paper by Kaplinghat, Tulin, and Yu [37] nicely summarizes a variety of constraints on dark electromagnetism models of SIDM. One point that is clear from Ref. [37] is that there exists only a narrow range of viable photon mixing parameters that can lead to production of SIDM in the early universe and interesting effects on cosmological structure formation, while simultaneously evading all constraints, including the constraint of Ref. [35]. Our results suggest that the SN1987A constraints from Ref. [35] are too restrictive. The constraints that we quote reveal a region of unrestricted mixing parameters that ranges over two orders of magnitude. Interestingly, the parameter space opened by our updated constraints corresponds to SIDM models that may have a significant impact on cosmological structure formation, particularly the structures of dark matter halos and galaxies.

The discrepancy between our result and that of Ref. [35] arises due to multiple factors. First, it is straightforward to demonstrate that the kinematical relationships in given in Appendix A of Ref. [35] are incorrect. Second, the squared matrix elements given in Eq. (A3) and Eq. (C18) of Ref. [35] are incorrect. Our squared matrix elements are considerably more complicated. Multiple errors must have led to the incorrect squared matrix elements in Ref. [35]. At the very least, these errors include simplification using the incorrect kinematics and neglect of the mass of the gauge boson (which, while legitimate for the  $\sim$ meV-mass axion, is not justified in this context). Discrepancies in addition to those kinematical issues must also be present, the causes of which are not apparent from the exposition, because the squared matrix elements in Eq. (A3) and Eq. (C18) of Ref. [35] do not obey the correct symmetries under interchange of the incoming or outgoing baryon momenta. Given these errors, we suggest that our results should

---

\*E-mail:cbm34@pitt.edu

†E-mail:akl2@pitt.edu

‡E-mail:zentner@pitt.edu

supercede these previously-published constraints.

The remainder of this paper is organized as follows. In Section II, we discuss dark photon models. We describe our calculation of SN1987A constraints on SIDM in Section III and present our primary results in Section IV. We summarize our work and draw conclusions in Section V.

## II. DARK PHOTON MODEL OF SIDM

[ARZ: Need to add citations to many of the Feng et al. papers here.] We consider constraints on SIDM specifically within the context of dark electromagnetism models. Dark electromagnetism models are models in which a hidden, dark, sector contains a broken  $U(1)'$  symmetry and the  $U(1)'$  gauge boson is kinetically mixed with the standard model photon. For the purposes of this study, this is important because it demands that the Lagrangian contains terms such as

$$\mathcal{L}_{\text{int}} = g_\chi \bar{\chi} \tilde{A}' \chi + q \bar{f} \tilde{A} f, \quad (1)$$

where  $\chi$  is the dark matter,  $g_\chi$  is the dark coupling,  $\tilde{A}'$  is the dark gauge boson,  $f$  is a standard model fermion of charge  $q$ , and  $\tilde{A}$  is the standard model gauge boson. The kinetic mixing, through a term  $\frac{1}{2} \frac{\varepsilon}{\sqrt{1+\varepsilon^2}} \tilde{F}_{\mu\nu} \tilde{F}'^{\mu\nu}$  in the Lagrangian causes the  $\tilde{A}$  to be an admixture of the massless photon  $A$ , and the dark photon  $A'$ , of mass  $m_{A'} = m_{\tilde{A}} \sqrt{1+\varepsilon^2} \simeq m_{\tilde{A}}$ , because the viable parameter range has  $\varepsilon \ll 1$ . The dark matter particles are thereby coupled to the standard model fermions with a coupling constant  $\varepsilon q$ , where  $\varepsilon$  is the kinetic mixing parameter. The first term in this interaction Lagrangian gives rise to the dark matter self-interactions.

Dark gauge bosons are produced in astrophysical environments such as supernova cores primarily via brehmsstrahlung off of standard model particles. This brehmsstrahlung occurs through the  $\varepsilon q$  coupling to charged standard model particles, in this particular case the proton and pion. The rate of brehmsstrahlung depends upon both  $\varepsilon$  and the mass of the  $A'$ . Consequently, supernova cooling can constrain the mixing  $\varepsilon$  as a function of  $m_{A'}$  for such models. Delineating such a constraint is the primary aim of this paper.

## III. METHODS

We aim to estimate the rate of energy loss from the core of a supernova from  $A'$  brehmsstrahlung during nucleon-nucleon interactions. The calculation is analogous to the well-known estimate of axion emission from supernova cores described in Ref. [34] and references therein, but

is more complicated because the mass of the  $A'$ , unlike the mass of the axion, is not necessarily negligible. This section describes the calculation of the rate of energy loss from a supernova core from  $A'$  brehmsstrahlung.

The brehmsstrahlung process is not the only process with which we must be concerned. Clearly, the rate of brehmsstrahlung will increase with  $\varepsilon$ ; however,  $\varepsilon$  can become sufficiently large that the radiated gauge bosons do not escape the supernova. This happens if the  $A'$  either decay to standard model particles or interact with standard model particles prior to exiting the supernova core. In either case, the energy is not lost and the  $A'$  does not provide a cooling channel for the supernova. Consequently, for a given  $m_{A'}$ , there is a maximum  $\varepsilon$  that can be constrained in this manner. We estimate  $A'$  decay and scattering probabilities, and the upper limits on the  $\varepsilon$  constraints in this section as well.

### A. Brehmsstrahlung of $A'$ Bosons

There are two processes to consider in order to estimate the rate of energy loss via  $A'$  brehmsstrahlung. The first is proton-proton (pp) scattering with the brehmsstrahlung of the dark photon off the proton;  $p + p \rightarrow p + p + A$ . The second is proton-neutron (pn) scattering with brehmsstrahlung off of either the proton or the charged pion;  $p + n \rightarrow p + n + A$ . We estimate the rates for these processes using the one-pion exchange (OPE) approximation for nucleon interactions. In the pp case, there are eight tree-level diagrams, with the emission of the  $A'$  from each of the external legs. One of these diagrams is shown in Fig. 1; the remaining seven diagrams come from placing the radiated  $A'$  on each of the other three protons and then, for each of these, interchanging the outgoing momenta. For the pn case, there are five diagrams, four of which are analogous to the pp diagram shown in Fig. 1. The fifth diagram, shown in Fig. 2, corresponds to emission of the  $A'$  from the exchanged, charged pion.

Evaluating these diagrams is tedious, but very straightforward. The calculation differs from the well-known axion brehmsstrahlung calculation, because the mass of the  $A'$  boson is not necessarily negligible in the kinematic region of interest for supernova explosions.

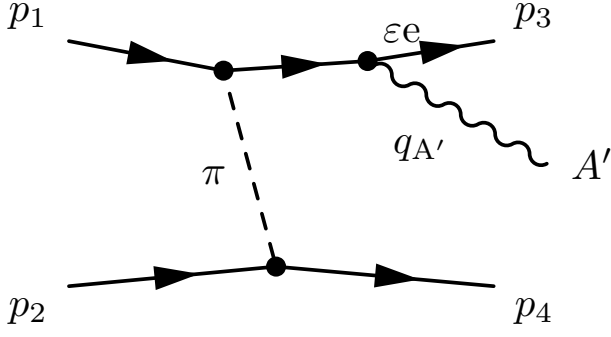


FIG. 1: One of the eight Feynman diagrams for the pp process. Three of the other diagrams are obtained by placing the  $A'$  on each of the protons in turn. The remaining four diagrams come from swapping the outgoing momenta.

The correct kinematical relations are

$$p_1 \cdot p_2 = M_N^2 - \frac{l^2}{2} - \frac{k^2}{2} + p_2 \cdot q_{A'}, \quad (2)$$

$$p_1 \cdot p_3 = M_N^2 + k \cdot l - \frac{k^2}{2} + p_3 \cdot q_{A'}, \quad (3)$$

$$p_1 \cdot p_4 = k \cdot l + M_N^2 - \frac{l^2}{2} + p_4 \cdot q_{A'}, \quad (4)$$

$$p_2 \cdot p_3 = M_N^2 - \frac{l^2}{2}, \quad (5)$$

$$p_2 \cdot p_4 = M_N^2 - \frac{k^2}{2}, \quad \text{and} \quad (6)$$

$$p_3 \cdot p_4 = k \cdot l + M_N^2 - \frac{l^2 + k^2}{2}, \quad (7)$$

where  $p_1$  and  $p_2$  are the four-momenta of the incoming nucleons,  $p_3$  and  $p_4$  are the momenta of the outgoing nucleons,  $q_{A'}$  is the  $A'$  momentum,  $k = p_2 - p_3$ ,  $l = p_2 - p_4$ , and  $M_N$  is the nucleon mass. These kinematical relations correct the relations in Ref. [35].

**[ARZ: Cameron, can you double check this? I think there were some errors in the momenta and in the relative signs of the diagrams. I tried to fix them. Please go over this carefully.]** The eight diagrams contribute the following eight terms to the pp amplitude,

$$M_1 = \frac{4M_N}{m_\pi} \frac{f_{\text{pp}}^2 e \varepsilon}{k^2 - m_\pi^2} \frac{1}{m_{A'}^2 - 2q_{A'} \cdot p_1} \bar{u}(p_4) \gamma_5 u(p_2) \bar{u}(p_3) \gamma_5 (\not{p}_1 - q_{A'} + M_N) \not{\varepsilon} u(p_1), \quad (8)$$

$$M_2 = -\frac{4M_N}{m_\pi} \frac{f_{\text{pp}}^2 e \varepsilon}{l^2 - m_\pi^2} \frac{1}{m_{A'}^2 - 2q_{A'} \cdot p_1} \bar{u}(p_3) \gamma_5 u(p_2) \bar{u}(p_4) \gamma_5 (\not{p}_1 - q_{A'} + M_N) \not{\varepsilon} u(p_1), \quad (9)$$

$$M_3 = \frac{4M_N}{m_\pi} \frac{f_{\text{pp}}^2 e \varepsilon}{l^2 - m_\pi^2} \frac{1}{m_{A'}^2 - 2q_{A'} \cdot p_2} \bar{u}(p_3) \gamma_5 u(p_1) \bar{u}(p_4) \gamma_5 (\not{p}_2 - q_{A'} + M_N) \not{\varepsilon} u(p_2), \quad (10)$$

$$M_4 = -\frac{4M_N}{m_\pi} \frac{f_{\text{pp}}^2 e \varepsilon}{k^2 - m_\pi^2} \frac{1}{m_{A'}^2 - 2q_{A'} \cdot p_2} \bar{u}(p_4) \gamma_5 u(p_1) \bar{u}(p_3) \gamma_5 (\not{p}_2 - q_{A'} + M_N) \not{\varepsilon} u(p_2), \quad (11)$$

$$M_5 = \frac{4M_N}{m_\pi} \frac{f_{\text{pp}}^2 e \varepsilon}{k^2 - m_\pi^2} \frac{1}{m_{A'}^2 + 2q_{A'} \cdot p_3} \bar{u}(p_3) \gamma_5 u(p_1) \bar{u}(p_4) \not{\varepsilon} (\not{p}_3 + q_{A'} + M_N) \gamma_5 u(p_2), \quad (12)$$

$$M_6 = -\frac{4M_N}{m_\pi} \frac{f_{\text{pp}}^2 e \varepsilon}{l^2 - m_\pi^2} \frac{1}{m_{A'}^2 + 2q_{A'} \cdot p_3} \bar{u}(p_4) \gamma_5 u(p_1) \bar{u}(p_3) \not{\varepsilon} (\not{p}_3 + q_{A'} + M_N) \gamma_5 u(p_2), \quad (13)$$

$$M_7 = \frac{4M_N}{m_\pi} \frac{f_{\text{pp}}^2 e \varepsilon}{k^2 - m_\pi^2} \frac{1}{m_{A'}^2 + 2q_{A'} \cdot p_4} \bar{u}(p_4) \gamma_5 u(p_2) \bar{u}(p_3) \not{\varepsilon} (\not{p}_4 + q_{A'} + M_N) \gamma_5 u(p_1), \quad (14)$$

$$M_8 = -\frac{4M_N}{m_\pi} \frac{f_{\text{pp}}^2 e \varepsilon}{l^2 - m_\pi^2} \frac{1}{m_{A'}^2 + 2q_{A'} \cdot p_4} \bar{u}(p_3) \gamma_5 u(p_2) \bar{u}(p_4) \not{\varepsilon} (\not{p}_4 + q_{A'} + M_N) \gamma_5 u(p_1), \quad (15)$$

where the dark photon polarization is given by  $\epsilon^\nu$ . The

squared amplitude is given by

$$|\mathcal{M}_{\text{pp}}|^2 = \sum_{s_1, s_2} \left| \sum_{i=1}^8 M_i \right|^2, \quad (16)$$

where the first summation is over the incoming proton polarizations. These expressions are identical to those given in Ref. [35]; however, they do not simplify significantly if the correct kinematics are used. Unfortunately, with the kinematical relations above, the squared amplitude does not yield a tidy expression for the spin-averaged squared matrix element. Our result contains over 200 terms, so we do not reproduce it here for rea-

sons of convenience. However, we note that our result for  $|\mathcal{M}_{pp}|^2$  is symmetric under exchange of  $k$  and  $l$  as required.

The pn process contain four diagrams analogous to the the diagrams for the pp process (there are only four, of course, because the neutrons cannot radiate the  $A'$ ). The new diagram that is relevant in the pn process is shown in Fig. 2 and yields a contribution of

$$M'_5 = \frac{4M_N}{m_\pi} \frac{f_{pn}^2 e \varepsilon}{l^2 - m_\pi^2} \frac{1}{(l - q_{A'})^2 - m_\pi^2} \bar{u}(p_3) \gamma_5 u(p_1) \bar{u}(p_4) \gamma_5 u(p_2) (q_{A'} - 2l) \cdot \varepsilon. \quad (17)$$

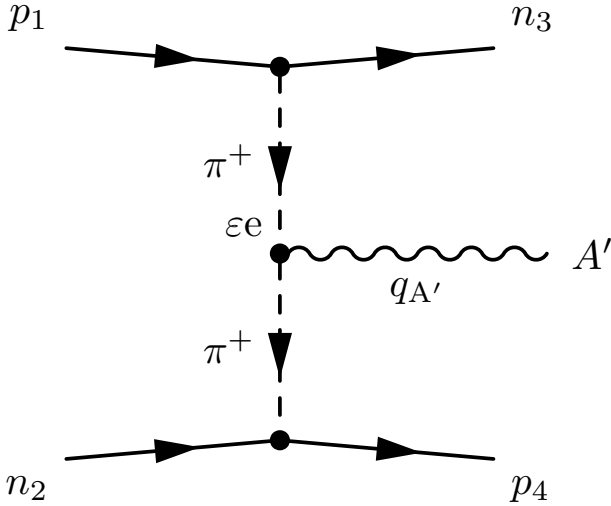


FIG. 2: One of the five Feynman diagrams for the np process. This particular diagram shows internal brehmsstrahlung off of the charged pion. The remaining four diagrams are analogous to the pp diagram shown in Fig. 1. In the case of the np processes, there are only four diagrams for brehmsstrahlung off of the external legs because two of the legs correspond to the uncharged neutron.

The pn processes likewise yield a squared amplitude,  $|\mathcal{M}_{pn}|^2$  that is unwieldy, so we do not give the the full

expression here.

### B. The Streaming Limit of the Energy Loss Rate

The first and simplest bound that may be obtained arises from assuming that all  $A'$  particles produced in the supernova core leave the supernova, carrying their energies with them. The constraint can be derived simply by requiring that the energy loss through this cooling channel be less than the cooling from neutrino emission; any greater, and it would have an observable effect on supernova cooling. This calculation yields values of  $\varepsilon$  above which cooling through  $A'$  production is too rapid to be consistent with SN1987A. We will consider modifications to this bound from  $A'$  trapping and decay in subsequent subsections.

The quantity of interest is the rate of energy emission through dark gauge bosons. From the spin-summed, squared amplitudes described in the previous subsection, the energy emission rate is obtained by integrating over the phase space, and adding a factor of the energy of the emitted particle. To be specific, the energy emission rate per unit volume is

$$Q_i = (2\pi)^4 \int E_{A'} \sum_{s_1, s_2} |\mathcal{M}_i|^2 f(p_1) f(p_2) \delta^{(4)}(p_1 + p_2 - p_3 - p_4 - q_{A'}) d\Pi, \quad (18)$$

where

$$d\Pi = \frac{d^3 \vec{q}_{A'}}{(2\pi)^3 2E_{A'}} \prod_{i=1}^4 \frac{d^3 \vec{p}_i}{(2\pi)^3 2E_i} \quad (19)$$

is the Lorentz-invariant phase space interval,  $E_{A'}$  is the energy of the emitted  $A'$  boson,  $f(p)$  are the phase-space densities of the incoming nucleons, and the index  $i$  refers

to either the pp or pn processes. The nucleons in the core are comfortably non-degenerate and non-relativistic, so the Pauli blocking factor is omitted from Eq. (18) and we take all nucleons to have a Maxwell-Boltzmann phase-space distribution distribution,

$$f(p) = \frac{n_b}{2} \left( \frac{2\pi}{M_N T} \right)^{3/2} \exp \left( -\frac{p^2}{2M_N T} \right). \quad (20)$$

We choose a baryon number density of  $n_b \approx 1.8 \times 10^{38} \text{ cm}^{-3}$  and a core supernova temperature of  $T = 30 \text{ MeV}$ , both of which are typical choices and thought to be representative of supernova cores. **[ARZ: Need to put a citation here for the properties of supernova cores. I can probably find something in the literature, but please put something here if you have a citation.]**

We performed the phase space integrals using the Monte Carlo routines in the CUBA library. **[ARZ: There needs to be some reference, citation, or some other information give about this library here.]** We integrated over the momenta  $\vec{p}_1, \vec{p}_2, \vec{p}_3$ , and the direction of the three-momentum of the radiated boson  $\hat{q}_{A'}$ , after fixing  $\vec{p}_4$  and the magnitude of  $\vec{q}_{A'}$  using the delta functions. **[ARZ: Cameron, can you double check this to be sure that it is correct? I rephrased it a bit, but I found the earlier phrasing to be a bit ambiguous and I can't remember which choice you made.]** We used the `suave` method provided within CUBA, which combines importance sampling and adaptive subdivision, as this method provided the best compromise between accuracy and run-time for this particular application.

To obtain the dark gauge boson luminosity from  $Q_{pp}$  and  $Q_{pn}$ , we assumed that  $A'$  production takes place in a stellar core of radius  $\sim 1 \text{ km}$ , so that the total luminosity of  $A'$  is

$$L_{A'} = V(Q_{pp} + Q_{pn}) \quad (21)$$

where  $V$  is the volume of the sphere. Clearly,  $L_{A'}$  is proportional to  $\varepsilon^2$ . Writing  $L_{A'} = \varepsilon^2 I_{A'}(m_{A'}, T)$ , as in Ref. [35], and  $L_\nu$  as the neutrino luminosity, we can write the constraint as

$$\varepsilon \lesssim \sqrt{\frac{L_\nu}{I_{A'}(m_{A'}, T)}}. \quad (22)$$

Following SOMEBODY **[ARZ: We need a citation here.]**, we derive a constraint taking  $L_\nu \approx 10^{53} \text{ erg/s} \approx 4 \times 10^{37} \text{ MeV}^2$ .

The constraint derived in this manner from Eq. (22) sets the lower limit on the exclusion band shown in Figure 3. We will discuss Fig. 3 in more detail below. If all of

the  $A'$  produced in the core leave the supernova freely, all values of  $\varepsilon$  higher than those given by Eq. (22) would be ruled out. However, as we have already mentioned,  $\varepsilon$  can become sufficiently large that only a negligible amount of energy actually exits the supernova core. For large values of  $\varepsilon$ , this can occur because of either  $A'$  decays or  $A'$  scattering. These additional considerations place an upper limit on the values of  $\varepsilon$  for which this constraint applies, and we discuss these effects in the next two subsections.

### C. The Decay Limit

The constraint from the streaming limit above provides an upper bound on the allowed coupling (or lower bound on the excluded coupling) from the production on  $A'$  bosons. In order to function as an effective cooling channel, enough of the dark gauge bosons must escape the supernova. As the coupling increases, so do processes that prevent this escape, and so the excluded region has an upper bound, above which the luminosity again drops below the neutrino luminosity. The first such limit may be found by considering decay of the dark bosons into Standard Model particles. Standard model particles will scatter and thermalize on a timescale much shorter than the timescale for the evolution of the core, so decays contribute nothing to the cooling.

The dark boson has a typical lifetime of **[ARZ: Cameron, try to rephrase this. This is not the lifetime, but rather the mean distance to a decay.]**

$$l = \frac{3E_A}{N_{eff} m_A^2 \varepsilon^2}, \quad (23)$$

and so the fraction escaping the supernova before decaying is given by

$$e^{r_{decay}/l} = e^{r_{decay} N_{eff} m_A^2 \varepsilon^2 / (3E_A)}. \quad (24)$$

To account for the suppression of gauge boson luminosity due to decays we simply multiply the phase space integrand in Eq. (18) by the exponential suppression factor, after which the calculation proceeds as in the previous subsection. The limit is derived in the same way, with the additional complication that  $I_{A'}$  is now a function of  $\varepsilon$ , in addition to  $m_{A'}$  and  $T$ . The constraint Eq. (22), therefore, becomes a transcendental equation that must be solved numerically.

The luminosity in  $A'$  will be an increasing function of  $\varepsilon$  until decays suppress the gauge boson luminosity, at which point  $L_{A'}$  becomes a rapidly decreasing function of  $\varepsilon$ . Therefore, the excluded values of  $\varepsilon$  at a given mass

will generally have a lower bound set by the calculations of the previous subsection, and an upper bound set by decays.

#### D. Trapping limit

**[ARZ: This section needs some work as it is a bit hard to follow.]** The second effect that produces an upper bound on the excluded region comes from considering trapping of dark bosons within the supernova. With a large enough coupling, the dark photons will thermalize and then will be emitted from an approximately spherical “dark photosphere” at the radial position where the  $A'$  mean free path becomes larger than the typical size of the supernova core. In this case the luminosity is given simply by Stefan’s law,

$$\mathcal{L}_t = 4\pi r^2 T_A^4 \sigma, \quad (25)$$

where  $r$  is now the radius of the emitting shell and  $T_A$  its temperature. We estimate the radius of this dark photosphere as  $r = 10$  km, because the density of the supernova drops drastically around that point. After taking that value for  $r$ , the bound on the luminosity translates into a bound on  $T_A$

$$T_A \leq 9.586 \text{ MeV}. \quad (26)$$

That bound can then be translated into the desired bound on the coupling as a function of mass by assuming that the particles are emitted from an optical depth  $\tau = 2/3$ , and finding the temperature that corresponds to that optical depth. This is a somewhat involved calculation. First, one needs a model for the density and temperature in the supernova. Following [35], we assume

$$\rho = \rho_p \left( \frac{R}{r} \right)^n, \quad (27)$$

$$T = T_R \left( \frac{\rho(r)}{\rho_R} \right)^{1/3}, \quad (28)$$

with  $\rho_p = 3 \times 10^{14} \text{ g/cm}^3$ ,  $T_R = 30 \text{ MeV}$ , and taking  $n = 5$ . The optical depth is given by

$$\tau = \int_{r_x}^{\infty} \kappa \rho dr, \quad (29)$$

where  $\kappa$  is the opacity. To find the opacity, we start from the reduced mean Rosseland opacity

$$\frac{1}{\kappa \rho} = \int_{m_x}^{\infty} \frac{15}{4\pi^4 T^5} \frac{E_A^2 e^{E_A/T} \sqrt{E_A^2 - m_A^2}}{(e^{E_A/T} - 1)^2} l_A dE_A, \quad (30)$$

where  $l_A$  is the mean free path.

The inverse mean free path can readily be obtained by modifying  $Q_i$ , the expression for the energy loss rate, as follows: removing the factor of  $E_A$  and the phase space integral over  $q_{A'}$ , and adding a factor of  $e^{E_A/T}$  for detailed balance. This gives the inverse mean free path as a function of mass and coupling. Again the required integration is performed numerically. This then allows the calculation of  $\kappa_x$ . The inverse opacities for the  $pn$  and  $pp$  processes add, giving the total opacity  $\kappa^{-1} = \kappa_{pp}^{-1} + \kappa_{pn}^{-1}$ .

Having obtained an expression for  $\kappa$ , we can now find the optical depth as follows: define a new quantity  $\tau_R = \kappa_R \rho_R R$ . We then have

$$\kappa \rho R = \tau_R \left( \frac{\rho}{\rho_R} \right)^2 \left( \frac{T_R}{T} \right)^{3/2} \quad (31)$$

This is combined with the expressions for the density and temperature as a function of  $r$  and plugged in to the integral expression for the optical depth to obtain

$$\tau_x = \int_{r_x}^{\infty} \tau_R \left( \frac{R}{r} \right)^{3n/2} \quad (32)$$

$$= \frac{\tau_R}{\frac{3n}{2} - 1} \left( \frac{T_A}{T_R} \right)^{(9/2 - 3/n)} \quad (33)$$

and the bound on the coupling is finally found by requiring  $\tau_x(\varepsilon, m_A) \leq 2/3$

#### E. Phase Space Integration

In every case

Once the integration is complete the calculation of the trapping and streaming limits is a straightforward application of the equations previously derived, and proceeded as outlined above. The decay limit is somewhat harder, since  $\varepsilon$  appears on both sides of the equation. Again we employed an unsubtle approach to solving the problem:  $\varepsilon$  was set to an arbitrary value where the constraint was satisfied, and then iteratively reduced until the constraint was no longer satisfied. This obviously introduces another source of error, but with a sufficiently small interval in  $\varepsilon$  this is negligible. The one further slight complication is that at after a certain value of  $M_A$  the decay limit rapidly goes to zero, at which point the procedure was terminated.

## IV. RESULTS

Let’s put some text here.



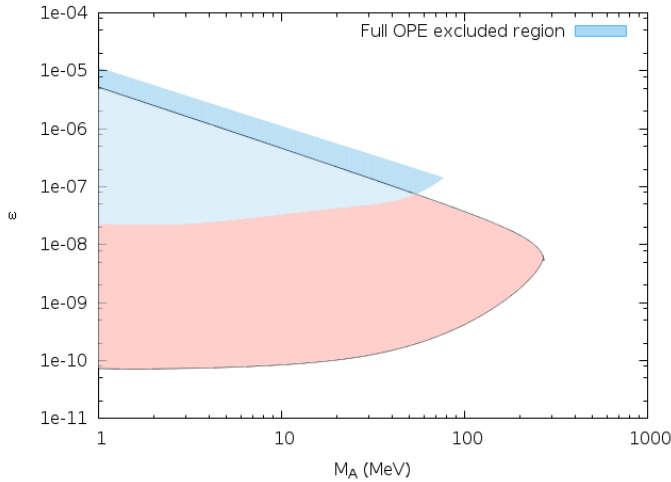


FIG. 3: A comparison of the final result for the excluded region with the result from Ref. [35]. The excluded region is clearly significantly less restrictive, and opens up the region of parameter space for  $\epsilon \approx 1e-8-9$ . [ARZ: Cameron, some similar comments as for Figure 1. Can we write numbers as "10<sup>-9</sup>" rather than "1e-09" and so on? Can we make the axis labels and tick mark labels larger?]

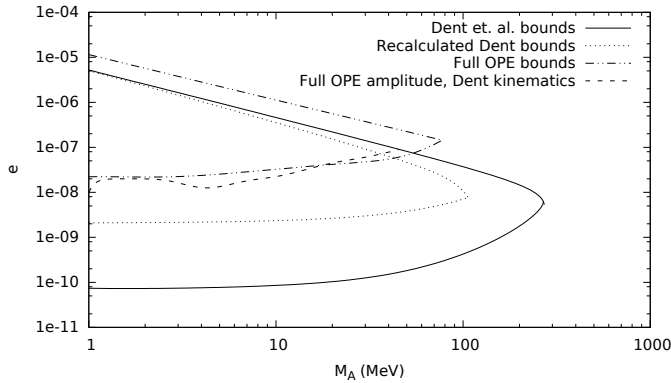


FIG. 4: The changes in the bounds generated as each stage of the calculation departs from Ref. [35]. Interestingly the kinematics have apparently relatively little effect. [ARZ: Cameron, several to-do items for this figure. On the y-axis, the symbol should be " $\epsilon$ " rather than "e". Can we write numbers as "10<sup>-9</sup>" rather than "1e-09" and so on? Can we make the axis labels and tick mark labels larger? Can you make all of the lines thicker? Can you make each of the four lines a distinct color?]

## V. DISCUSSION AND CONCLUSIONS

The revised approach produce constraints that are significantly weaker than the previous work, and that largely reproduce constraints already obtained from beam dump experiments.

### Acknowledgments

AKL was supported in part by NSF grant PHY-1519175.

- 
- [1] G. Jungman, M. Kamionkowski, and K. Griest, Phys. Reports **267**, 195 (1996).
  - [2] E. D. Carlson, M. E. Machacek, and L. J. Hall, Astro-phys. J. **398**, 43 (1992).
  - [3] A. A. de Laix, R. J. Scherrer, and R. K. Schaefer, Astro-

- phys. J. **452**, 495 (1995), arXiv:astro-ph/9502087.
- [4] F. Atrio-Barandela and S. Davidson, Phys. Rev. D **55**, 5886 (1997), arXiv:astro-ph/9702236.
- [5] D. N. Spergel and P. J. Steinhardt, Phys. Rev. Lett. **84**, 3760 (2000), arXiv:astro-ph/9909386.

- [6] C. J. Hogan and J. J. Dalcanton, Phys. Rev. D **62**, 063511 (2000), arXiv:astro-ph/0002330.
- [7] R. N. Mohapatra and V. L. Teplitz, Phys. Rev. D **62**, 063506 (2000), arXiv:astro-ph/0001362.
- [8] R. Davé, D. N. Spergel, P. J. Steinhardt, and B. D. Wandelt, Astrophys. J. **547**, 574 (2001), arXiv:astro-ph/0006218.
- [9] J. Hisano, S. Matsumoto, and M. M. Nojiri, Phys. Rev. Lett. **92**, 031303 (2004), arXiv:hep-ph/0307216.
- [10] J. Hisano, S. Matsumoto, M. M. Nojiri, and O. Saito, Phys. Rev. D **71**, 063528 (2005), arXiv:hep-ph/0412403.
- [11] M. Pospelov, A. Ritz, and M. Voloshin, Phys. Lett. B **662**, 53 (2008), 0711.4866.
- [12] N. Arkani-Hamed, D. P. Finkbeiner, T. R. Slatyer, and N. Weiner, ArXiv e-prints (2008), 0810.0713.
- [13] M. Lattanzi and J. Silk, ArXiv e-prints (2008), 0812.0360.
- [14] L. Ackerman, M. R. Buckley, S. M. Carroll, and M. Kamionkowski, Phys. Rev. D **79**, 023519 (2009), 0810.5126.
- [15] J. L. Feng, M. Kaplinghat, H. Tu, and H.-B. Yu, Journal of Cosmology and Astro-Particle Physics **7**, 4 (2009), 0905.3039.
- [16] K. Kong, G. Mohlabeng, and J.-C. Park, Physics Letters B **743**, 256 (2015), 1411.6632.
- [17] N. Yoshida, V. Springel, S. D. M. White, and G. Tormen, Astrophys. J. Lett. **544**, L87 (2000), arXiv:astro-ph/0006134.
- [18] O. Y. Gnedin and J. P. Ostriker, Astrophys. J. **561**, 61 (2001), arXiv:astro-ph/0010436.
- [19] J. Miralda-Escudé, Astrophys. J. **564**, 60 (2002).
- [20] S. W. Randall, M. Markevitch, D. Clowe, A. H. Gonzalez, and M. Bradač, Astrophys. J. **679**, 1173 (2008), 0704.0261.
- [21] M. Kamionkowski and S. Profumo, Phys. Rev. Lett. **101**, 261301 (2008).
- [22] A. R. Zentner, Phys. Rev. D **80**, 063501 (2009), 0907.3448.
- [23] B. E. Robertson and A. R. Zentner, Phys. Rev. D **79**, 083525 (2009), 0902.0362.
- [24] L. Pieri, M. Lattanzi, and J. Silk, ArXiv e-prints (2009), 0902.4330.
- [25] D. Spolyar, M. Buckley, K. Freese, D. Hooper, and H. Murayama, ArXiv e-prints (2009), 0905.4764.
- [26] D. P. Finkbeiner, T. Lin, and N. Weiner, ArXiv e-prints (2009), 0906.0002.
- [27] T. R. Slatyer, N. Padmanabhan, and D. P. Finkbeiner, ArXiv e-prints (2009), 0906.1197.
- [28] J. Bramante, K. Fukushima, J. Kumar, and E. Stopnitzky, Phys. Rev. D **89**, 015010 (2014), 1310.3509.
- [29] I. F. M. Albuquerque, C. Pérez de los Heros, and D. S. Robertson, J. Cosmol. Astropart. Phys. **2**, 047 (2014), 1312.0797.
- [30] M. Kaplinghat, S. Tulin, and H.-B. Yu, Phys. Rev. D **89**, 035009 (2014), 1310.7945.
- [31] C.-S. Chen, F.-F. Lee, G.-L. Lin, and Y.-H. Lin, J. Cosmol. Astropart. Phys. **10**, 049 (2014), 1408.5471.
- [32] J. L. Feng, J. Smolinsky, and P. Tanedo, Phys. Rev. D **93**, 115036 (2016).
- [33] R. Catena and A. Widmark, J. Cosmol. Astropart. Phys. **12**, 016 (2016), 1609.04825.
- [34] G. G. Raffelt, *Stars as laboratories for fundamental physics : the astrophysics of neutrinos, axions, and other weakly interacting particles* (University of Chicago Press, 1996).
- [35] J. B. Dent, F. Ferrer, and L. M. Krauss, ArXiv e-prints (2012), 1201.2683.
- [36] E. Rrapaj and S. Reddy, Phys. Rev. C **94**, 045805 (2016), 1511.09136.
- [37] M. Kaplinghat, S. Tulin, and H.-B. Yu, ArXiv e-prints (2013), 1308.0618.